Integrative Analyses of Key Genes Associated With Carotid Atherosclerosis Plaque Stability

Zhenyu Guo
Department of Vascular Surgery, Qingpu Branch of Zhongshan Hospital, Fudan University
Baixue Yu
Biomedical Research Centre, Zhongshan Hospital, Fudan University
Tao Wang
Department of Vascular Surgery, Qingpu Branch of Zhongshan Hospital, Fudan University
Xiaohu Yang
Department of Vascular Surgery, Qingpu Branch of Zhongshan Hospital, Fudan University
Chen Wang
Department of Vascular Surgery, Zhongshan Hospital, Fudan University
Longhua Fan (longhuafanzs@126.com)
Department of Vascular Surgery, Qingpu Branch of Zhongshan Hospital, Fudan University

Research Article

Keywords: Carotid plaque rupture, Kyoto Encyclopedia of Genes and Genomes (KEGG), gene ontology (GO)

Posted Date: December 10th, 2020

DOI: https://doi.org/10.21203/rs.3.rs-121154/v1

Abstract

Carotid plaque rupture with thrombosis is responsible for the majority of acute cerebrovascular events. The study aimed to identify key genes associated with plaque destabilization. In our study, expression profiles regarding carotid plaque stability (GSE41571 and GSE120521) were obtained from the Gene Expression Omnibus (GEO) database and used to analyze differentially expressed genes (DEGs), key biological processes (BP) and intersecting pathways. And the expression of the DEGs was validated in clinical and cell samples. A total of 113 DEGs were identified and gene ontology (GO) analysis and Kyoto Encyclopedia of Genes and Genomes (KEGG) analysis were performed. Among the BP annotations, changes in “extracellular matrix (ECM) were closely related to plaque stability. “Focal adhesion”, ECM - receptor interaction”, “vascular smooth muscle contraction” and “regulation of actin cytoskeleton” were key pathways associated with plaque stability. Genes with top 15 scores (CytoHubba) were selected as hub genes, including ACTA2, MYLK, CALD1, MYH10, ACE, HMOX1, CYBA, NOX4, LUM, RAC2, COL4A5, SDC1, UCP2, SORBS1, and FCER1G. Pathway enrichment analysis showed that selected hub genes were also significantly enriched in “vascular smooth muscle contraction” and “focal adhesion”. Further detection in tissue and cell samples suggested MYLK, NOX4, COL4A5, SDC1 and CYBA might have potential clinical significance.

Introduction

Ischemic stroke has become one of the world's leading causes of morbidity, mortality and disability, and affects more than 690,000 people in the United States each year.[1] And in China, the annual stroke mortality rate reaches nearly 1.6 million, which puts a great burden on patients’ quality of life and healthcare expenditures.[2] The occurrence and development of ischemic stroke are determined by the interaction of many factors, among which the formation of atherosclerotic plaques is an important pathogenic factor.[3]

Atherosclerosis mainly affects large and medium-sized arteries and especially occurs in organs such as the heart, brain, and kidney.[4] The pathogenesis of atherosclerosis is characterized by a smoldering vascular inflammatory disease driven by lipids, involving early lesions (pathological intimal thickening and intimal xanthoma) and advanced plaque (thin or thick fibrous cap atheroma).[5]

Histological analyses proposed two types of atherosclerotic plaques based on carotid plaque morphology, including stable and unstable plaques.[5] Stable plaques are characterized by a thick fibrous cap, accompanied by macroscopic calcification. By contrast, unstable plaques or rupture-prone plaques have been shown to have typical pathological features and histological evidence of vulnerability, including a thin overlying fibrous cap and an obvious necrotic core, with inflammatory cell infiltration, intra-plaque hemorrhage, and regional calcification.[6] Rupture of carotid plaques and the consequent thrombosis is considered the main cause of acute cerebrovascular events[5,7]. Therefore, elucidating the

mechanism of unstable plaque formation and exploring underlying biomarkers are essential for the prevention of ischemic stroke.

In our research, we obtained the gene expression profile data from the public GEO database. The study aimed to investigate significant potential genes associated with atherosclerotic plaque destabilization and gain a deeper insight into the pathogenesis and progression of atherosclerosis.

Results

DEGs identification After data normalization (Fig. 1A and B), principal component analysis (PCA) was performed to compare the differences between stable and unstable plaques (Fig. 1C and D). 779 upregulated genes and 750 downregulated genes were identified in the two databases, with 113 overlapping DEGs (Fig. 1E, F and G).

Functional and Pathway Enrichment of DEGs The online tool DAVID v6.8 was used to extract and summarize functional annotation associated with DEGs (Table I). GO analysis revealed BP terms of the DEGs were significantly enriched in phagocytosis, ECM organization, positive regulation of B cell activation and cell adhesion and inflammatory response; cellular component (CC) terms mainly enriched in the proteinaceous ECM, extracellular exosome, extracellular region, ECM and extracellular space; molecular function (MF) terms mainly enriched in calcium ion binding, heparin binding, collagen binding, immunoglobulin receptor binding and actin binding. KEGG pathway enrichment analysis demonstrated DEGs were closely related to focal adhesion, ECM-receptor interaction, chemokine signaling pathway, vascular smooth muscle contraction, regulation of actin cytoskeleton and regulation of lipolysis in adipocytes.

PPI Network Analysis The protein-protein direct (physical) and indirect (functional) associations were analyzed with the STRING database to construct a PPI network (Fig. 2A). The data were further uploaded into Cytoscape to visualize molecular interaction networks. CytoHubba was used to predict key nodes in the PPI network, and genes ranking top 15 (maximum correlation criterion) were selected as hub genes (Fig. 2B), namely actin alpha 2 smooth muscle (ACTA2), Myosin light chain kinase (MYLK), Caldesmon1 (CALD1), myosin heavy chain 10 (MYH10), Angiotensin-converting enzyme (ACE), Heme oxygenase 1 (HMOX1), cytochrome b-245 alpha chain (CYBA), NADPH oxidase 4 (NOX4), lumican (LUM), Rac family small GTPase 2 (RAC2), collagen type IV alpha 5 chain (COL4A5), Syndecan-1 (SDC1), uncoupling protein 2 (UCP2), Sorbin and SH3 domain-containing protein 1 (SORBS1), Fc fragment of IgE receptor Ig (FCER1G).

Hub gene functional Enrichment Functional and pathway enrichment analyses were performed to explore the biological classification of 15 hub genes (Table II). In the BP categories, hub genes were mainly enriched in muscle contraction, response to hypoxia, cellular response to glucose stimulus, regulation of blood pressure, superoxide anion generation and superoxide metabolic process. In CC categories, hub genes were mainly enriched in stress fiber, focal adhesion, lamellipodium, plasma membrane, NADPH oxidase complex and external side of the plasma membrane. In MF categories, hub genes were mainly

enriched in actin binding, heme binding, superoxide-generating NADPH oxidase activity, calmodulin binding, extracellular matrix structural constituent and electron carrier activity. Pathway enrichment analysis revealed 15 hub genes were significantly associated with vascular smooth muscle contraction and focal adhesion.

Validation of Hub Genes by RT-qPCR Demographic and clinical data of patients was shown in Table III. The results showed that hub genes, including MYLK, NOX4, COL4A5 and SDC1, were downregulated in unstable plaques compared with that in stable plaques (Fig. 2C). In contrast, the expression of CYBA in the unstable plaques was significantly upregulated. Consistent with the mRNA results of carotid plaques, the expression levels of MYLK, NOX4, COL4A5 and SDC1 were also decreased in HASMCs treated with ox-LDL. Besides, and the expression differences were also found in CYBA, ACTA2, CALD1, HMOX1, LUM, RAC2, UCP2, SORBS1 and FCER1G (Fig. 2D).

Prediction of potential miRNA Genes validated previously were selected and potential miRNAs were predicted with miRWalk 3.0, TargetScan and miRTarBase. The mRNA-miRNA interaction network was processed with Cytoscape 3.8.1 (supplementary Fig. 1). The analysis revealed hsa-miR-373-3p targeted both MYLK and SDC1.

Discussion

Emerging studies reported the occurrence of stroke is closely related to the nature and structure of carotid atherosclerotic plaques, and the prevalence of ischemic stroke in unstable plaques is significantly higher than that in stable plaques.[8,9] Early identification of rupture-prone plaques can help recognize patients at high risk of stroke, who may derive a benefit from early revascularization. In the present study, a comprehensive analysis of GEO datasets (GSE41571 and GSE120521) was conducted to explore crucial DEGs between stable and unstable plaques and a total of 113 DEGs were identified. The DAVID database was used to perform gene enrichment analysis, and results revealed these genes were mainly involved in the changes of ECM organization and vascular smooth muscle contraction. Furthermore, 15 hub genes were identified and the enrichment analysis result also highlighted the pathways including vascular smooth muscle contraction and focal adhesion. The screened hub genes were further validated in carotid plaque and vascular smooth muscle cell (VSMCs) samples, and the results revealed MYLK, NOX4, COL4A5, SDC1 and CYBA may have potential clinical values.

Atherosclerosis has been known as a maladaptive chronic lipid-driven inflammatory lesion, with dysfunction of endothelial cells (ECs) barrier function as the initiating steps.[10] EC dysfunction is mainly characterized by increased expression levels of inflammatory cytokines and permeability, which allows lipid particles to accumulate and infiltrate in ECM and initiates an inflammatory cascade reaction.[11] The dysfunctional ECs and modified ECM induced monocyte recruitment, adhesion and transmigration, which then differentiate into macrophages and constitute the necrotic core by internalizing lipid particles.[12] Concurrently, the migration of VSMCs and abnormally secreted ECM contributed to the formation of the fibrous cap.

Among BP and CC annotations (Table I), the changes in ECM were closely related to the progression of plaque stability. The disorder of ECM was implicated in the pathogenesis of the atherogenic process, and changes in matrix protein have been reported to be related to atherosclerotic complications, including vascular calcification and plaque rupture[13–15]. The composition of ECM proteins changes significantly during atherosclerotic plaque formation, which is primarily synthesized and excreted by VSMCs, fibroblasts and macrophages.[16] Besides, these cells also expressed ECM-degrading enzymes, including cathepsins, tryptase, and matrix metalloproteinases (MMPs)[16]. Aberrant expression of ECM-degrading enzymes could lead to a reduction in the amount of matrix component, and fragmentation of ECM. The uncontrolled ECM degradation contributes to the gradual weakening of fibrous caps and leads to an instability predisposition.[16,17] The role of MMPs in the collagenolysis has attracted much attention. MMPs are a family of zinc-dependent ECM degrading proteinases, which act a critical role in different stages of atheromatous plaque.[18] Among the MMPs family, MMP-9 (gelatinase) has been widely studied due to potential pro-atherogenic properties. Multiple studies have confirmed that patients with unstable plaques have higher levels of circulating MMP-9 than those with stable plaques, indicating a potential link between MMP-9 and atherosclerotic plaque destabilization.[19] The findings were further supported by overexpression of MMP-9 in macrophages, which exhibited several manifestations correlated with plaque destabilization in apoE-deficient mice.[13]

In addition, enrichment analysis data of hub genes were highly consistent with the results of DEGs. Both analysis results highlighted focal adhesion and vascular smooth muscle contraction pathways. In normal arterial walls, VSMCs are characterized as a quiescent contractile phenotype. During the atherogenic process, VSMCs could transform into a proliferative secretory phenotype.[14] The migratory VSMCs and secreted collagen constitute the main component of the fibrous cap and are responsible for plaque stability and tensile strength. Accordingly, loss of VSMCs leads to undesirable effects. Ox-LDL has been recognized as a crucial factor for atherogenesis and could induce the apoptosis and death of VSMCs, accompanied by resultant thinning of the fibrous cap.[20] VSMCs of the secretory phenotype is also the primary source of MMPs in atherosclerotic lesions, which in turn promote matrix degradation, fibrous cap weakening and plaque destabilization.[21]

Focal adhesion kinase (FAK) is known as a protein tyrosine kinase, involved in cell adhesion, migration, proliferation and apoptosis.[22] FAK is predominantly localized in nuclei of VSMCs. Increased matrix deposition contributes to the activation of FAK, which promotes VSMC proliferation and vascular remodeling.[23] In addition, the activation of FAK has been implicated in cytoskeletal recombination, indicating a potential link between FAK and changes in vascular contractility. Among the 15 hub genes, most genes were closely correlated with VSMC contractility, including ACTA2, MYLK, CALD1, MYH10 and NOX4. The final result of verification also demonstrated a significant reduction in these contractility-related genes (Fig. 2C and D).

Increased reactive oxygen species (ROS) has proven to be a risk factor for atherogenesis, and NADPH oxidase complexes serve as the major source of ROS.[24] The enrichment analysis of hub genes also

revealed a change in NADPH oxidase complexes, among which NOX4 was identified to be downregulated in rupture-prone lesions and ox-LDL-treated HASMCs (Fig. 2C and D). NOX4 is required for the maintenance of the VSMC contractile phenotype.[25] In contrast to other NOX members, NOX4 is constitutively active and primarily generate H_2O_2 rather than superoxide. Due to the incapability to scavenge nitric oxide, low constitutive H_2O_2 generated by NOX4 was therefore thought to be beneficial in atherogenesis and has anti-atherosclerotic functions.[26,27]

MiRNAs have emerged as a key player in the biological process. With the ability to regulate post-transcriptional gene expression, the effect of miRNAs on the initiation and development of atherosclerosis has attracted more attention.[28,29] In our study, we predicted the potential miRNAs of hub genes and observed that hsa-miR-373-3p targeted both MYLK and SDC1, which were involved in signaling pathways including focal adhesion, ECM-receptor interaction, and vascular smooth muscle contraction. The results revealed hsa-miR-373-3p was implicated in the progression of atherosclerosis and may be of potential value in evaluating the severity of atherosclerotic diseases.

The study still had some limitations. First, the study was limited by a relatively small number of cases. Only 11 plaque samples were analyzed from the GEO datasets. Secondly, due to a lack of clinical data in corresponding GEO datasets, there might be some biases imposed by other risk factors. Therefore, the results should be interpreted with caution. Third, further study was needed to explore the role of hub genes and hsa-miR-373-3p in the progression of atherosclerotic diseases.

Conclusion

Carotid plaque rupture with resultant thrombosis is responsible for the majority of acute ischemic stroke. Our study was performed to identify the key genes associated with the ruptured traits of atheromatous plaques. Further detection suggested MYLK, NOX4, COL4A5, SDC1 and CYBA might have potential clinical significance.

Materials And Methods

Ethics statement Studies involving human samples were approved by the ethics committee of the Qingpu Branch of Zhongshan Hospital, affiliated with Fudan University (2020-54). All procedures conformed to the principles outlined in the Declaration of Helsinki and written informed consents were obtained from all patients before enrollment in the present study.

Data Source and preprocessing GEO is an international public functional genomics data repository (https://www.ncbi.nlm.nih.gov/geo/). Two gene expression datasets (GSE41571 and GSE120521) were selected from GEO based on the following inclusion criteria: (1) Homo sapiens (Organism); (2) carotid atherosclerotic plaque; (3) samples including stable plaque and unstable plaque. The raw data were obtained from the GEO data repository, followed by background correction and data normalization in the R software (version 4.0.2).

Screening of Differentially Expression Genes (DEGs)and enrichment analysis DEGs analysis was performed by R package limma as previously described.[30] $|\log_2$ fold change (FC)$|>1$ and $P < 0.05$ served as the threshold to identify the potential DEGs. Functional enrichment analyses of screened DEGs, including GO terms (BP, CC and MF) and KEGG pathway analyses, were conducted via DAVID online database (https://david.ncifcrf.gov/). $P < 0.05$ was regarded as cut-off criteria for statistical significance.

PPI network Analysis The STRING database (https://string-db.org/, Version 11.0) was applied to methodically analyze the biological functions of screened DEGs and functional interactions between proteins.[31] Cytoscape (version 3.8.1), an open-source software platform[32], was used for network data integration, analysis and visualization. In addition, the hub genes were further analyzed by CytoHubba (a Cytoscape plugin) as previously described.[33]

Hub genes pathway enrichment analyses and prediction of potential microRNA The hub genes identified previously were submitted to DAVID online database to perform functional and pathway enrichment analysis. $P < 0.05$ was considered statistically significant. MiRWalk 3.0 (http://mirwalk.umm.uni-heidelberg.de/) was used to predict the corresponding miRNA with a 3'UTR binding site.[34] The predicted results were further verified by other databases (TargetScan and miRTarBase). The final miRNAs at the intersection were selected and Cytoscape 3.8.1 was used to visualize the miRNA-mRNA network.

Sample collection Human carotid artery plaque samples were collected from patients receiving carotid endarterectomy between June 2020 and October 2020. Preoperative Doppler ultrasound examinations were performed for all participants to assess carotid plaque vulnerability.[35] The diagnosis of carotid artery stenosis was further determined using computerized tomography angiography. Pathological specimens after the operation (including 5 stable and 5 unstable plaques) were immediately stored in liquid nitrogen for the following analysis.

Cell culture Human aortic smooth muscle cells (HASMCs) were obtained from ScienCell Research Laboratories, Inc. and cultured with smooth muscle cell medium (ScienCell).

Human oxidized modified low-density lipoprotein (ox-LDL, Yiyuan Biotechnologies, Guangzhou, China) was added into the cell culture medium (0, 25 and 50 ug/ml) for 24 hours.[36] Cells exposed to corresponding conditions were then collected to explore the expression levels of related genes.

Real-time quantitative polymerase chain reaction (RT-qPCR) The total RNA was extracted from tissues or cell samples using TRIzol RNA Isolation Reagents (Invitrogen, Carlsbad, Calif). The following reverse transcription was performed using Hifair® □ 1st Strand cDNA Synthesis SuperMix (Yeasen Biotech Co., Ltd., Shanghai, China). Afterward, based on ABI QuantStudio 5 Real-Time PCR System (Thermo Fisher Scientific Inc.), the real-time quantitative polymerase chain reaction was conducted with Hieff® qPCR SYBR Green Master Mix (Yeasen Biotech Co., Ltd.) under the manufacturer's instructions. Human GAPDH was applied as an endogenous calibrator to compare the expression levels of targeted genes. The relative

quantification of mRNA expression levels was analyzed using the $2^{-\triangle\triangle Ct}$ formula. Primer sequences of targeted genes were listed in Supplementary Table I.

Statistical analysis Data were presented as mean ± standard deviations or absolute numbers and further analyzed by Student t-test or Fisher's exact test (SPSS 24.0). $P < 0.05$ was considered statistically significant.

Declarations

Acknowledgments

The study was supported by grants from the Shanghai Natural Science Foundation (20ZR1411800).

Author Contributions

Conceived and designed the study: Z.Y.G., B.X.Y., T.W. and L.H.F.;

Searched databases: Z.Y.G., B.X.Y., and X.H.Y.;

Data analyses: Z.Y.G., B.X.Y., and C.W;

Preparation of tables and figures: Z.Y.G., B.X.Y., and X.H.Y.;

Wrote and revised the manuscript: Z.Y.G., B.X.Y., X.H.Y. and L.H.F.;

All authors reviewed the manuscript.

Competing Interests: The authors declare no competing interests.

References

1. Kernan, W. N. *et al.* Guidelines for the prevention of stroke in patients with stroke and transient ischemic attack: a guideline for healthcare professionals from the American Heart Association/American Stroke Association. *Stroke* **45**, 2160–2236, doi:10.1161/STR.0000000000000024 (2014).
2. Liu, L., Wang, D., Wong, K. S. & Wang, Y. Stroke and stroke care in China: huge burden, significant workload, and a national priority. *Stroke* **42**, 3651–3654, doi:10.1161/strokeaha.111.635755 (2011).
3. Berntsson, J. *et al.* Orosomucoid, Carotid Plaque, and Incidence of Stroke. *Stroke* **47**, 1858–1863, doi:10.1161/strokeaha.116.013374 (2016).
4. Weber, C. & Noels, H. Atherosclerosis: current pathogenesis and therapeutic options. *Nat. Med.* **17**, 1410–1422, doi:10.1038/nm.2538 (2011).
5. Bentzon, J. F., Otsuka, F., Virmani, R. & Falk, E. Mechanisms of plaque formation and rupture. *Circ. Res.* **114**, 1852–1866, doi:10.1161/circresaha.114.302721 (2014).

6. Andrews, J. P. M., Fayad, Z. A. & Dweck, M. R. New methods to image unstable atherosclerotic plaques. *Atherosclerosis* **272**, 118–128, doi:10.1016/j.atherosclerosis.2018.03.021 (2018).
7. Butcovan, D., Mocanu, V., Baran, D., Ciurescu, D. & Tinica, G. Assessment of vulnerable and unstable carotid atherosclerotic plaques on endarterectomy specimens. *Exp. Ther. Med.* **11**, 2028–2032, doi:10.3892/etm.2016.3096 (2016).
8. Saba, L. *et al.* Imaging biomarkers of vulnerable carotid plaques for stroke risk prediction and their potential clinical implications. *Lancet. Neurol.* **18**, 559–572, doi:10.1016/s1474-4422(19)30035-3 (2019).
9. Pelisek, J., Eckstein, H. H. & Zernecke, A. Pathophysiological mechanisms of carotid plaque vulnerability: impact on ischemic stroke. *Arch. Immunol. Ther. Exp. (Warsz)* **60**, 431–442, doi:10.1007/s00005-012-0192-z (2012).
10. Schaftenaar, F., Frodermann, V., Kuiper, J. & Lutgens, E. Atherosclerosis: the interplay between lipids and immune cells. *Curr. Opin. Lipidol.* **27**, 209–215, doi:10.1097/mol.0000000000000302 (2016).
11. Hansson, G. K., Libby, P. & Tabas, I. Inflammation and plaque vulnerability. *J. Intern. Med.* **278**, 483–493, doi:10.1111/joim.12406 (2015).
12. Moore, K. J. & Tabas, I. Macrophages in the pathogenesis of atherosclerosis. *Cell* **145**, 341–355, doi:10.1016/j.cell.2011.04.005 (2011).
13. Johnson, J. L. Metalloproteinases in atherosclerosis. *Eur. J. Pharmacol.* **816**, 93–106, doi:10.1016/j.ejphar.2017.09.007 (2017).
14. Bennett, M. R., Sinha, S. & Owens, G. K. Vascular Smooth Muscle Cells in Atherosclerosis. *Circ. Res.* **118**, 692–702, doi:10.1161/circresaha.115.306361 (2016).
15. Lanzer, P. *et al.* Medial vascular calcification revisited: review and perspectives. *Eur. Heart. J.* **35**, 1515–1525, doi:10.1093/eurheartj/ehu163 (2014).
16. Reimann, C. *et al.* Molecular imaging of the extracellular matrix in the context of atherosclerosis. *Adv. Drug. Deliv. Rev.* **113**, 49–60, doi:10.1016/j.addr.2016.09.005 (2017).
17. Chistiakov, D. A., Sobenin, I. A. & Orekhov, A. N. Vascular extracellular matrix in atherosclerosis. *Cardiol. Rev.* **21**, 270–288, doi:10.1097/CRD.0b013e31828c5ced (2013).
18. Sakakura, K. *et al.* Pathophysiology of atherosclerosis plaque progression. *Heart. Lung. Circ.* **22**, 399–411, doi:10.1016/j.hlc.2013.03.001 (2013).
19. Kobayashi, N. *et al.* Matrix Metalloproteinase-9 as a Marker for Plaque Rupture and a Predictor of Adverse Clinical Outcome in Patients with Acute Coronary Syndrome: An Optical Coherence Tomography Study. *Cardiology* **135**, 56–65, doi:10.1159/000445994 (2016).
20. Grootaert, M. O. J. *et al.* Vascular smooth muscle cell death, autophagy and senescence in atherosclerosis. *Cardiovasc. Res.* **114**, 622–634, doi:10.1093/cvr/cvy007 (2018).
21. Cui, N., Hu, M. & Khalil, R. A. Biochemical and Biological Attributes of Matrix Metalloproteinases. *Prog. Mol. Biol. Transl. Sci.* **147**, 1–73, doi:10.1016/bs.pmbts.2017.02.005 (2017).

22. Zhao, X. & Guan, J. L. Focal adhesion kinase and its signaling pathways in cell migration and angiogenesis. *Adv. Drug. Deliv. Rev.* **63**, 610–615, doi:10.1016/j.addr.2010.11.001 (2011).
23. Jeong, K. *et al.* Nuclear Focal Adhesion Kinase Controls Vascular Smooth Muscle Cell Proliferation and Neointimal Hyperplasia Through GATA4-Mediated Cyclin D1 Transcription. *Circ. Res.* **125**, 152–166, doi:10.1161/circresaha.118.314344 (2019).
24. Nowak, W. N., Deng, J., Ruan, X. Z. & Xu, Q. Reactive Oxygen Species Generation and Atherosclerosis. *Arterioscler. Thromb. Vasc. Biol.* **37**, e41-e52, doi:10.1161/atvbaha.117.309228 (2017).
25. Clempus, R. E. *et al.* Nox4 is required for maintenance of the differentiated vascular smooth muscle cell phenotype. *Arterioscler. Thromb. Vasc. Biol.* **27**, 42–48, doi:10.1161/01.atv.0000251500.94478.18 (2007).
26. Craige, S. M. *et al.* Endothelial NADPH oxidase 4 protects ApoE-/- mice from atherosclerotic lesions. *Free Radic. Biol. Med.* **89**, 1–7, doi:10.1016/j.freeradbiomed.2015.07.004 (2015).
27. Langbein, H. *et al.* NADPH oxidase 4 protects against development of endothelial dysfunction and atherosclerosis in LDL receptor deficient mice. *Eur. Heart. J.* **37**, 1753–1761, doi:10.1093/eurheartj/ehv564 (2016).
28. Lu, Y., Thavarajah, T., Gu, W., Cai, J. & Xu, Q. Impact of miRNA in Atherosclerosis. *Arterioscler. Thromb. Vasc. Biol.* **38**, e159-e170, doi:10.1161/atvbaha.118.310227 (2018).
29. Laffont, B. & Rayner, K. J. MicroRNAs in the Pathobiology and Therapy of Atherosclerosis. *Can. J. Cardiol.* **33**, 313–324, doi:10.1016/j.cjca.2017.01.001 (2017).
30. Ritchie, M. E. *et al.* limma powers differential expression analyses for RNA-sequencing and microarray studies. *Nucleic. Acids. Res.* **43**, e47, doi:10.1093/nar/gkv007 (2015).
31. Szklarczyk, D. *et al.* STRING v10: protein-protein interaction networks, integrated over the tree of life. *Nucleic. Acids. Res.* **43**, D447-452, doi:10.1093/nar/gku1003 (2015).
32. Smoot, M. E., Ono, K., Ruscheinski, J., Wang, P. L. & Ideker, T. Cytoscape 2.8: new features for data integration and network visualization. *Bioinformatics* **27**, 431–432, doi:10.1093/bioinformatics/btq675 (2011).
33. Chin, C. H. *et al.* cytoHubba: identifying hub objects and sub-networks from complex interactome. *BMC. Syst. Biol.* **8 Suppl 4**, S11, doi:10.1186/1752-0509-8-s4-s11 (2014).
34. Dweep, H., Sticht, C., Pandey, P. & Gretz, N. miRWalk–database: prediction of possible miRNA binding sites by "walking" the genes of three genomes. *J. Biomed. Inform.* **44**, 839–847, doi:10.1016/j.jbi.2011.05.002 (2011).
35. Cloutier, G. *et al.* Carotid Plaque Vulnerability Assessment Using Ultrasound Elastography and Echogenicity Analysis. *AJR. Am. J. Roentgenol.* **211**, 847–855, doi:10.2214/ajr.17.19211 (2018).
36. Song, Y. *et al.* TLR4/NF-κB/Ceramide signaling contributes to Ox-LDL-induced calcification of human vascular smooth muscle cells. *Eur. J. Pharmacol.* **794**, 45–51, doi:10.1016/j.ejphar.2016.11.029 (2017).

Tables

Table I. GO and KEGG pathway enrichment analysis of DEGs

Category	Pathway ID	Pathway	Count	P Value
GOTERM_BP_DIRECT	GO:0006911	phagocytosis, engulfment	7	9.07E-08
GOTERM_BP_DIRECT	GO:0030198	extracellular matrix organization	9	4.15E-05
GOTERM_BP_DIRECT	GO:0050871	positive regulation of B cell activation	4	6.20E-04
GOTERM_BP_DIRECT	GO:0006910	phagocytosis, recognition	4	7.74E-04
GOTERM_BP_DIRECT	GO:0007155	cell adhesion	11	8.05E-04
GOTERM_BP_DIRECT	GO:0006954	inflammatory response	10	8.09E-04
GOTERM_CC_DIRECT	GO:0005578	proteinaceous extracellular matrix	14	6.68E-09
GOTERM_CC_DIRECT	GO:0070062	extracellular exosome	40	1.04E-07
GOTERM_CC_DIRECT	GO:0005576	extracellular region	29	1.40E-07
GOTERM_CC_DIRECT	GO:0031012	extracellular matrix	12	1.47E-06
GOTERM_CC_DIRECT	GO:0005615	extracellular space	24	3.23E-06
GOTERM_CC_DIRECT	GO:0030027	lamellipodium	8	4.68E-05
GOTERM_MF_DIRECT	GO:0005509	calcium ion binding	15	1.14E-04
GOTERM_MF_DIRECT	GO:0008201	heparin binding	7	4.43E-04
GOTERM_MF_DIRECT	GO:0005518	collagen binding	5	4.90E-04
GOTERM_MF_DIRECT	GO:0034987	immunoglobulin receptor binding	4	5.18E-04
GOTERM_MF_DIRECT	GO:0003779	actin binding	8	0.001571799
GOTERM_MF_DIRECT	GO:0003823	antigen binding	5	0.003640555
KEGG_PATHWAY	hsa04510	Focal adhesion	6	0.009643946
KEGG_PATHWAY	hsa04512	ECM-receptor interaction	4	0.017819247
KEGG_PATHWAY	hsa04062	Chemokine signaling pathway	5	0.030289347
KEGG_PATHWAY	hsa04270	Vascular smooth muscle contraction	4	0.038333964
KEGG_PATHWAY	hsa04810	Regulation of actin cytoskeleton	5	0.044267629
KEGG_PATHWAY	hsa04923	Regulation of lipolysis in adipocytes	3	0.049525017

Table II. GO and KEGG pathway enrichment analysis of hub genes

Category	Pathway ID	Pathway Description	Count	P Value
GOTERM_BP_DIRECT	GO:0006936	muscle contraction	4	8.70E-05
GOTERM_BP_DIRECT	GO:0001666	response to hypoxia	4	3.54E-04
GOTERM_BP_DIRECT	GO:0071333	cellular response to glucose stimulus	3	8.36E-04
GOTERM_BP_DIRECT	GO:0008217	regulation of blood pressure	3	1.30E-03
GOTERM_BP_DIRECT	GO:0042554	superoxide anion generation	2	1.16E-02
GOTERM_BP_DIRECT	GO:0006801	superoxide metabolic process	2	1.66E-02
GOTERM_CC_DIRECT	GO:0001725	stress fiber	5	6.74E-08
GOTERM_CC_DIRECT	GO:0005925	focal adhesion	5	1.76E-04
GOTERM_CC_DIRECT	GO:0030027	lamellipodium	4	2.25E-04
GOTERM_CC_DIRECT	GO:0005886	plasma membrane	9	5.39E-03
GOTERM_CC_DIRECT	GO:0043020	NADPH oxidase complex	2	9.18E-03
GOTERM_CC_DIRECT	GO:0009897	external side of plasma membrane	3	1.13E-02
GOTERM_MF_DIRECT	GO:0003779	actin binding	5	6.33E-05
GOTERM_MF_DIRECT	GO:0020037	heme binding	3	5.58E-03
GOTERM_MF_DIRECT	GO:0016175	superoxide-generating NADPH oxidase activity	2	9.09E-03
GOTERM_MF_DIRECT	GO:0005516	calmodulin binding	3	1.04E-02
GOTERM_MF_DIRECT	GO:0005201	extracellular matrix structural constituent	2	0.054175
GOTERM_MF_DIRECT	GO:0009055	electron carrier activity	2	0.072135
KEGG_PATHWAY	hsa04270	Vascular smooth muscle contraction	3	0.016936
KEGG_PATHWAY	hsa04510	Focal adhesion	3	0.04835

Table III. Demographic and clinical data of patients

Variables	Stable group (n=5)	Unstable group (n=5)	P Value
Age (years)	60.6±5.81	63.8±12.6	0.62
Male: female	3:2	1:4	0.52
Hypertension (n)	2	4	0.52
Diabetes (n)	2	2	1.00
hyperlipidemia (n)	4	3	1.00
coronary artery disease (n)	1	3	0.52

Figures

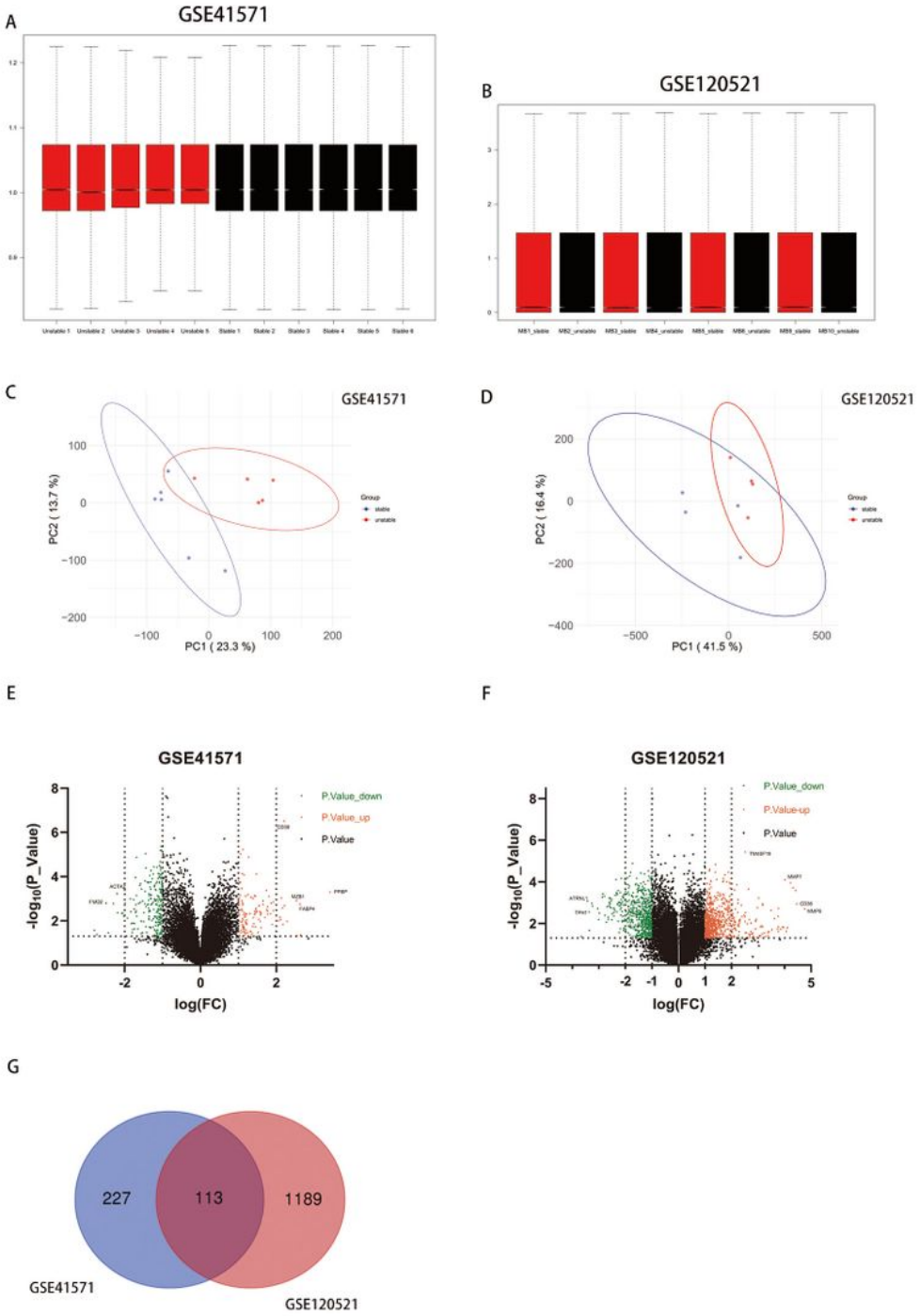

Figure 1

Sample preprocessing and DEGs identification. A, data normalization between stable and unstable plaques in GSE41571. B, data normalization in GSE120521. C, PCA of gene expression between stable and unstable plaques in GSE41571. D, PCA of gene expression in GSE120521. E, distributions of DEGs in GSE41571, with dark dots representing no significantly changed genes. F, distributions of DEGs in GSE120521. G, the intersection genes from GSE41571 and GSE120521 shown in Venn diagram.

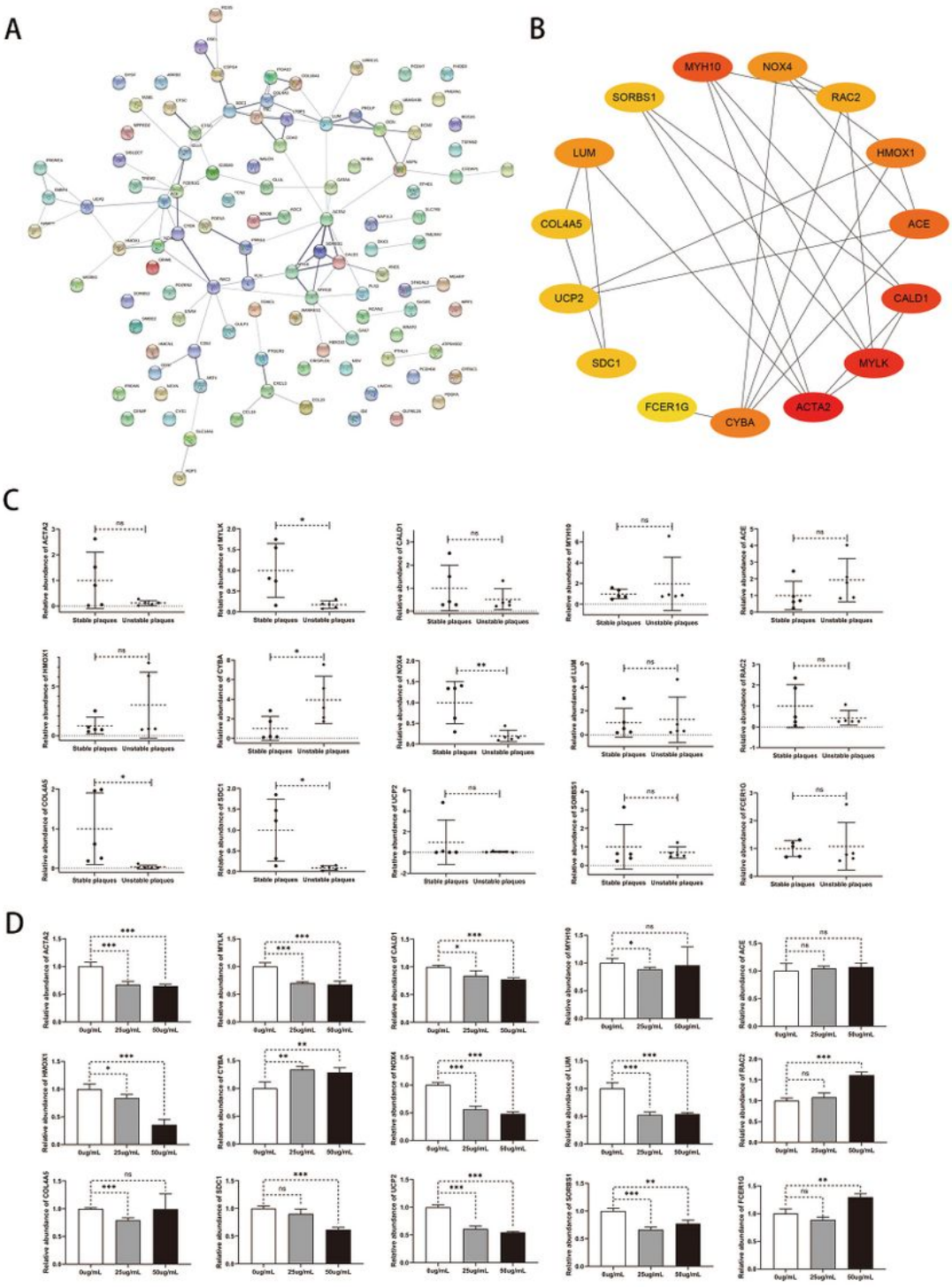

Figure 2

Key genes screening and validation. A, PPI network for 113 intersection genes from GSE41571 and GSE120521, with the nodes and lines representing corresponding proteins and interactions between the proteins. B, the 15 hub genes analyzed with maximum correlation criterion (the redder colors representing more forward ranking). C, validation of the hub genes in stable and unstable plaque samples. D, validation of the hub genes in ox-LDL-treated VSMCs.

Supplementary Files

This is a list of supplementary files associated with this preprint. Click to download.

- SupplementaryInformation.pdf